Food and Applied Bioscience Journal, 2020, 8(3): 1–18

Application of agricultural waste activated carbon prepared from sugarcane leaves for methyl orange removal in aqueous solution

Suchada Sawasdee*, Saleewiew Suwanputa, Chawalit Seesaiya, Sirilak Sritotesporn, Nattinan Tosri, Natnicha Sawangsup, Rattikan Pumpikun and Prachart Watcharabundit

Abstract

The aim of this work was to prepare activated carbon from sugarcane leaves for methyl orange dye adsorption from aqueous solution. The characterization methods of the adsorbent such as Fourier Transform Infrared Spectroscopy (FTIR), Scanning Electron Microscopy (SEM), and Brunauer–Emmett–Teller (BET) were evaluated. Batch adsorption experiments were carried out at varying conditions such as pH (4–10), contact time (5–300 min), adsorbent dose (0.2–1.0 g), initial dye concentration (20–100 mg/L), and temperature (20–40°C). The equilibrium adsorption data were analyzed by Langmuir and Freundlich isotherm models. The kinetic adsorption data were analyzed by pseudo–first order, pseudo-second order, and intra-particle diffusion models. The experimental results showed that the maximum percentage of dye adsorption found at pH 4 was 83.54. The equilibrium adsorption data were fitted well by the Freundlich isotherm, and the maximum adsorption capacity was found to be 12.50 mg/g at 30°C. For the kinetics of adsorption, the data were well described by the pseudo–second–order model at all temperatures. Moreover, the thermodynamic parameter showed that the adsorption process was spontaneous at 40°C and the process was endothermic in nature. The results indicated that the activated carbon could be employed as a low–cost effective adsorbent for dye adsorption from aqueous solution.

Keyword: Adsorption, methyl orange, sugarcane leaves, activated carbon

Department of Chemistry, Faculty of Science and Technology, Thepsatri Rajabhat University, Lopburi, 15000

**Corresponding author. E–mail: ps_neng@hotmail.com*

Received: 27 February 2020, Accepted: 14 July 2020

Food and Applied Bioscience Journal, 2020, 8(3): 1–18

1. Introduction

Water is one of the necessities for the living of life, but the increased industrial and agricultural activities have resulted in pollution of natural water resources. Synthetic dyes are widely used in many industries such as textile, leather, plastic, food processing, cosmetics, paper, printing, pharmaceutical and dye manufacturing (Chen *et al.,* 2010). Dyes are synthetic aromatic water-soluble organic colorants and difficult to treat because they are recalcitrant pollutants, resistant to aerobic digestion, and stable when exposed to oxidizing agents (Daneshvar *et al.,* 2014). The presence of dyes can cause damage to living beings in water because it is able to reduce both photosynthetic activity and dissolution of oxygen. Many methods such as flocculation, chemical coagulation, precipitation, ion exchange, photochemical degradation, biological degradation, chemical oxidation, reverse osmosis, flotation, and adsorption have been used for the removal of dyes from aqueous solutions (Khan *et al.,* 2011 and Chen *et al.,* 2010). Adsorption method is popular due to its simplicity and an effective process for removal of non-biodegradable pollutants, including dyes, from wastewater (Sharma *et al.,* 2010).

Activated carbon is used as the adsorbent to remove dyes from water due to its significant adsorption capacity. However, its use is limited because of the high cost adsorbent (Sharma and Kaur, 2011). The activation of a carbonaceous precursor can be performed through physical (steam, air or CO_2) or chemical activation (KOH, K_2CO_3, $ZnCl_2$, and H_3PO_4). The KOH activation enhances the specific surface area and the formation of –OH functional groups on the carbon surface (Hui and Zaini., 2015).

At present, there is a great interest in searching inexpensive and effective alternatives to the existing commercial activated carbon. Waste materials have been conducted for the preparation of activated carbon, including cotton stalk (Deng *et al.,* 2010), pineapple peel (Foo and Hameed, 2012), and gulfweed (Li *et al.,* 2017).

The main objective of this study was to investigate the methyl orange adsorption in batch process onto activated carbon prepared from sugarcane leaves. The effects of dye adsorption at varying pH (4–10), contact time (5–300 min), adsorbent dose (0.2–1.0 g), initial dye concentration (20–100 mg/L), and temperature (20–40°C) were evaluated. This adsorbent was characterized by BET, FTIR and SEM. The equilibrium adsorption data were analyzed using Langmuir and Freundlich isotherm models. The kinetic adsorption data were analyzed by the pseudo-first-order, pseudo-second-order, and intraparticle diffusion models. Thermodynamic parameters such as ΔG, ΔH, and ΔS were also evaluated.

Food and Applied Bioscience Journal, 2020, 8(3): 1–18

2. Materials and Methods

2.1 Preparation of activated carbon

The sugarcane leaves used in this study were obtained from a sugarcane plantation from Khok Samrong District, Lopburi Province, Thailand. The sugarcane leaves were washed thoroughly by tap water to remove any soil, dust and impurities. They were dried in a hot oven at 80°C for 6 h, cut to about 1–2 inches, and soaked for 4 h in 3.0 M KOH with impregnation ratio of 1 : 15 (g:cm^3), and carbonized at 300°C for 1 h. Then, the activated carbon material was washed with water to remove residual KOH until pH 7, and it was dried in a hot air oven. The dried adsorbent was powdered and sieved particle size to 150–300 µm, then, it was stored in a desiccator until used.

2.2 Characterization of adsorbent

The surface area of the adsorbent was determined by BET method. The surface functional group of adsorbent was analyzed by Fourier transform infrared spectrometer (FTIR, Perkin Elmer, model two) and the spectra were recorded from 4000–750 cm^{-1}. The surface morphology of the adsorbent was studied by the scanning electron microscope (SEM).

2.3 Preparation of adsorbate

Methyl orange was dried at 80°C for 2 h before using. The chemical structure of methyl orange is shown in Fig 1 (Chen *et al.,* 2010). The stock solution was prepared by dissolving a constant mass of dye in double distilled water to achieve the concentration of 500 mg/L and subsequently diluted to the required concentrations. All chemicals and reagents used were of analytical grade (HCl and NaOH) and commercial grade (KOH).

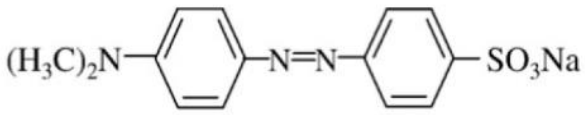

Fig 1 Chemical structure of methyl orange dye

2.4 Batch adsorption study

Batch adsorption was carried out by known amount of adsorbent with 100 mL of dye solution in 250–mL Erlenmeyer flasks. Adsorption studies were performed at varying conditions of pH (4–10), contact time (5–300 min), adsorbent dose (0.2–1.0 g), initial dye concentration (20–100 mg/L), and temperature (20–40°C). The pH of the dye solution was adjusted by 0.1 M HCl and 0.1 M NaOH. The flasks of mixture between dye solution and adsorbent were maintained under an isothermal shaker and agitation speed of 200 rpm. At the end of shaking time for each flask, the suspended matter was filtered and the supernatant was measured for

Food and Applied Bioscience Journal, 2020, 8(3): 1–18

dye concentration by UV–Visible spectrophotometer at 465 nm. The percentage of adsorption and amount of adsorption capacity (q_t) were calculated as follows:

$$\% \text{ adsorption} = \frac{(C_o - C_t)}{C_o} \times 100 \quad (1)$$

$$q_t = \frac{(C_o - C_t)V}{W} \quad (2)$$

where C_o (mg/L) is initial dye concentration, C_t (mg/L) is the concentration at any time, q_t (mg/g) is the amount adsorbed at any time, V(L) is the volume of the solution, and W(g) is the mass of adsorbent.

2.5 Adsorption Isotherm

To optimize the design of the adsorption process, it is important to establish the most appropriate correlation for the equilibrium curves. The adsorption isotherm indicates how adsorbate molecules are distributed between the solid and liquid phases when the adsorption process is in an equilibrium state.

The Langmuir isotherm in a linear form is represented as follows (Foo and Hameed, 2012):

$$\frac{C_e}{q_e} = \frac{1}{q_m} C_e + \frac{1}{K_L q_m} \quad (3)$$

Where C_e (mg/L) is the equilibrium concentration, q_e (mg/g) is the adsorption capacity at equilibrium, K_L is the Langmuir constant, and q_m (mg/g) is the maximum adsorption capacity.

The essential characteristics of a Langmuir isotherm can be expressed in terms of a dimensionless separation factor (R_L) which is defined by:

$$R_L = \frac{1}{(1 + K_L C_o)} \quad (4)$$

The value of R_L indicates the shape of the isotherm to be either unfavorable (R_L>1), linear (R_L = 1), and favorable (0 < R_L< 1) or irreversible (R_L = 0).

The Freundlich isotherm in a linear form is represented as follows (Foo and Hameed, 2012):

$$\log q_e = \log K_F + 1/n \log C_e \quad (5)$$

Where K_F (L/g) is the adsorption capacity and 1/n is the adsorption intensity.

Food and Applied Bioscience Journal, 2020, 8(3): 1–18

2.6 Adsorption kinetics

The pseudo first–order and pseudo second–order models in a linear form are written as follows:

$$\log (q_e - q_t) = \log q_e - \frac{k_1}{2.303} t \quad (6)$$

$$\frac{t}{q_t} = \frac{1}{k_2 q_e^2} + \frac{1}{q_e} t \quad (7)$$

where k_1 (min^{-1}) and k_2 ($g.mg^{-1}.min^{-1}$) are the rate constant of pseudo–first order and pseudo-second order.

The intraparticle diffusion model is expressed as:

$$q_t = k_{id} t^{1/2} + C \quad (8)$$

Where q_t is the adsorption capacity at any time of adsorbate, k_{id} is the rate constant ($mg/g\ min^{1/2}$), and C is the intercept explaining for the thickness of boundary layer.

2.7 Thermodynamic study

The thermodynamic parameters namely, Gibbs free energy (ΔG), enthalpy change (ΔH), and entropy change (ΔS) were evaluated. The Gibbs free energy change (ΔG) is related to the adsorption equilibrium constant (K) and it can be expressed as follows:

$$\Delta G = -RT \ln K \quad (9)$$

where K (= q_e / C_e) is the equilibrium constant, R is the gas constant (8.314 J/moL.K), and T is the absolute temperature (K). The enthalpy change (ΔH) and entropy change (ΔS) can be expressed as follows:

$$\log (q_e / C_e) = \frac{\Delta S}{2.303R} - \frac{\Delta H}{2.303RT} \quad (10)$$

The values of ΔH and ΔS are determined from slope and intercept of the plot of log (q_e / C_e) versus 1/T.

3. Results and Discussion

3.1 Characterization of adsorbent

For Fig 2, the textural structure of activated carbon by SEM showed the present porous and large number of rough surface.

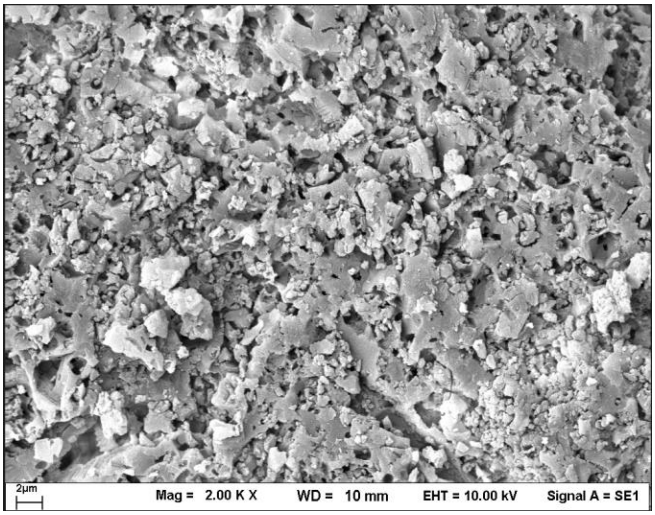

Fig 2 SEM of KOH–activated carbon from sugarcane leaves.

The BET surface area and the total pore volumes of the obtained KOH–sugarcane leaf activated carbon were found to be 26.95 m^2/g and 0.0530 cm^3/g, respectively.

The FT–IR spectra of KOH–activated carbon before and after dye adsorption were recorded in the range of 4,000-750 cm^{-1} as shown in Fig 3. The bands around 3100–3600 cm^{-1} were due to the stretching vibrations of the hydroxyl functional groups (OH) (Saad *et al.,* 2019). The peaks at 2250-2400 cm^{-1} denote C=O stretching from ketones, aldehydes or carboxylic groups in the raw samples and the interaction between oxygen and carbon during pyrolysis in the activated carbon. Oxygen-containing surface functional groups play an important role in influencing the surface properties and adsorption behavior of the adsorbents, though adsorbents were prepared via the different activation methods (Alau *et al.,* 2015). FTIR spectra results indicated the presence of oxygen–containing surface functional groups such as hydroxyl groups, ketones, aldehydes, lactones or carboxyl groups in the activated carbon adsorbent. Moreover, there was a significant change in the wavenumber of before and after adsorption spectra.

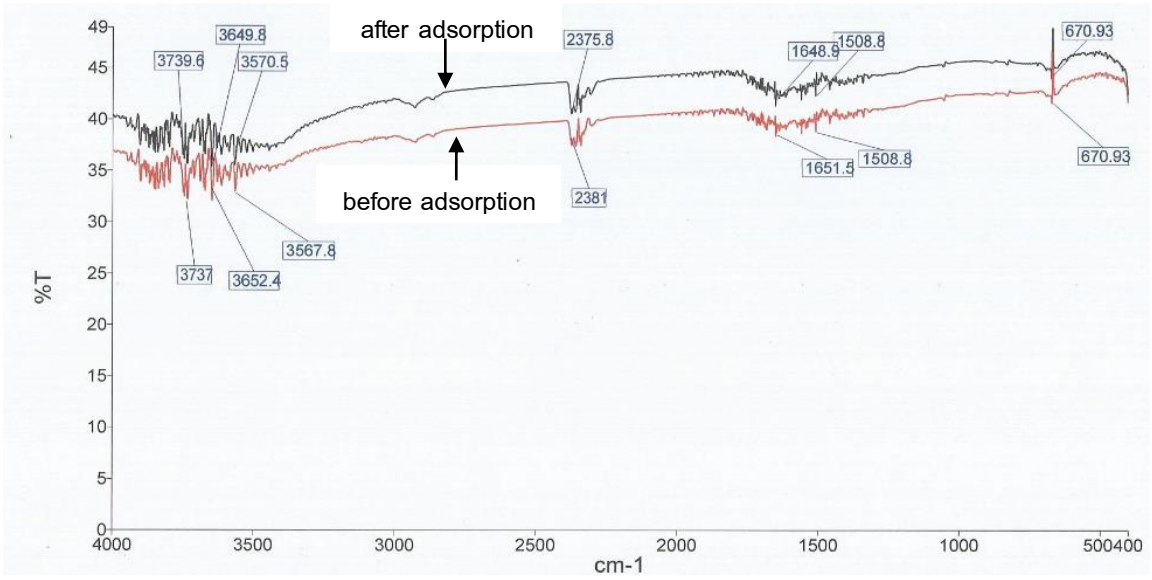

Fig 3 FT−IR spectrum of activated carbon before and after dye adsorption

3.2 Effect of pH

The pH played an important role on the adsorption capacity. The dye adsorption was studied at pH 4 to 10 for the initial dye concentration at 20 mg/L, and the percentage of adsorption was shown in Fig 4. At pH less than 4.0, the experiment could not be investigated because of color change of dye solution (Bamroongwongdee *et al.,* 2018). The results showed that the percentage of adsorption decreased from 83.54% to 15.30% when the pH value of the dye solution increased from 4 to 10. The maximum percentage of dye adsorption (83.54%) was found at pH 4, because the electrostatic attraction existed on the positively charged surface of the adsorbent and anionic dye. This could be explained that the functional groups of the adsorbent would be protonated at low pH, which was necessary for the attraction of anionic dye molecules. The adsorption was drastically decreased at pH over 4. At higher pH (>4), more OH^- would available to compete with the anionic dye molecules for the adsorption on the surface of adsorbent, thus the adsorption of dye decreased. Mechanism of dye adsorption could be presented as Equation (11) and Equation (12):

$$Ac-COOH + H^+ \leftrightarrow Ac\text{-}CO\ OH_2^+ \quad \text{.....(11)}$$

$$Ac-COOH_2^+ + OH_2^+ + Dye - SO_3^- \leftrightarrow Ac-COOH_2^+\ SO_3^-\text{-}Dye \text{.....(12)}$$

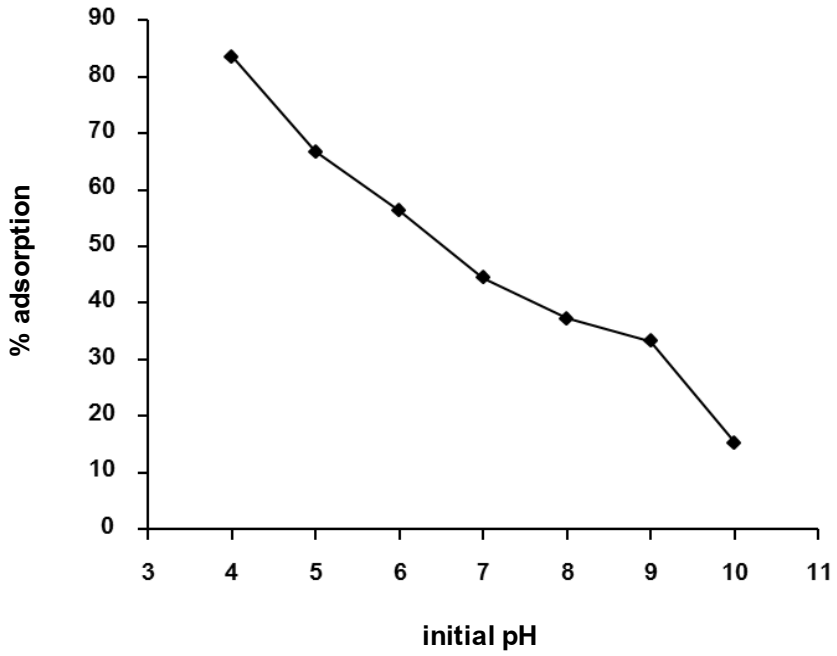

Fig 4 Effect of pH on dye adsorption

3.3 Effect of contact time

The effect of contact time (5–300 min) on adsorption was studied for the initial dye concentration of 20 mg/L, at pH 4 and at different temperatures (20–40℃). The plots of adsorption capacity versus contact time were shown in Fig 5 As seen in Fig 5, the adsorption rate was rapid at the first 15 min and then gradually decreased with time until reached the equilibrium at 120 min at all temperatures. From 5 to 120 min, the adsorption capacity increased from 0.674 to 1.565 mg/g, 0.730 to 1.671 mg/g, and 0.941 to 1.753 mg/g at 20, 30 and 40℃, respectively. The adsorption capacity increased as the temperature increased because of the enlargement of pore size and activation of the sorbent surface with temperature (Pathania *et al.,* 2017), leading to fast diffusion of dye molecules across the external boundary layer and internal pore structure of the adsorbent particles (Albroomi *et al.,* 2017). In conclusion, it is due to the increased interaction between dye molecules and adsorbent surface at higher temperature.

The initial rapid stage adsorption observed during the first 15 min was probably due to the abundant availability of active sites on the adsorbent surface (Shao *et al.,* 2017). With the increase in contact time, the rate of adsorption decreased. This may be attributed to the lack of available active sites required for further uptake after attaining the equilibrium (Pathania *et al.,* 2017 and Liang *et al.,* 2010). In addition, the adsorption capacity increased with an increase in the temperature, indicating that the adsorption was endothermic process (Chen *et al.,* 2010).

Similar observations have been reported as Chen *et al.,* (2010), Ai *et al.* (2011), and Yu *et al.* (2018).

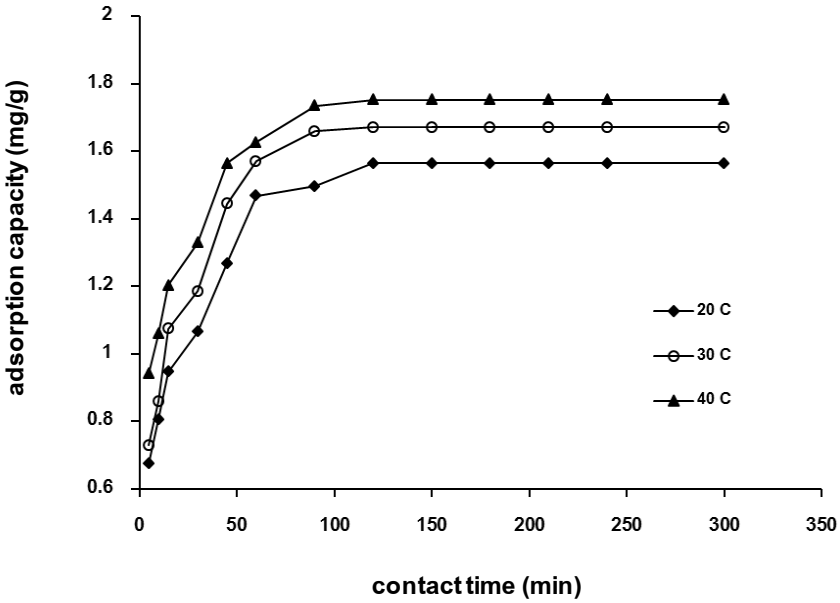

Fig 5 Effect of contact time on dye adsorption

3.4 Effect of adsorbent dose

The effect of adsorbent dose (0.2 – 1.0 g) on dye adsorption onto activated carbon was studied for the initial dye concentration of 20 mg/L at pH 4. The results in Fig 6 presented that the percentage of adsorption valued 33.83 to 83.54% with increased in adsorbent dose (0.2 – 1.0 g) due to increase number of adsorption sites at the higher amount of adsorbent. In addition, at higher adsorbent dose the percentage of adsorption kept increasing gradually until became constant. This may be attributed to overlapping of adsorption sites resulting in decrease in total surface area available to dye (Crini *et al.,* 2007) and (Jayganesh *et al*., 2018). The similar observation has been reported by Ngulube *et al.* (2018). On the other hand, the adsorption capacity decreased from 3.384 to 1.671 mg/g with increased adsorbent dose from 0.2 to 1.0 g due to competition or overlapping between the methyl orange molecules, which were bound to the available adsorption sites of the adsorbent Yu *et al.* (2018), and it was due to overlapping of adsorption sites while increasing adsorbent dose (Nsami and Mbadcam, 2013). The similar observations have been reported by other researchers such as Yu *et al.* (2018) and Yokout *et al.* (2019).

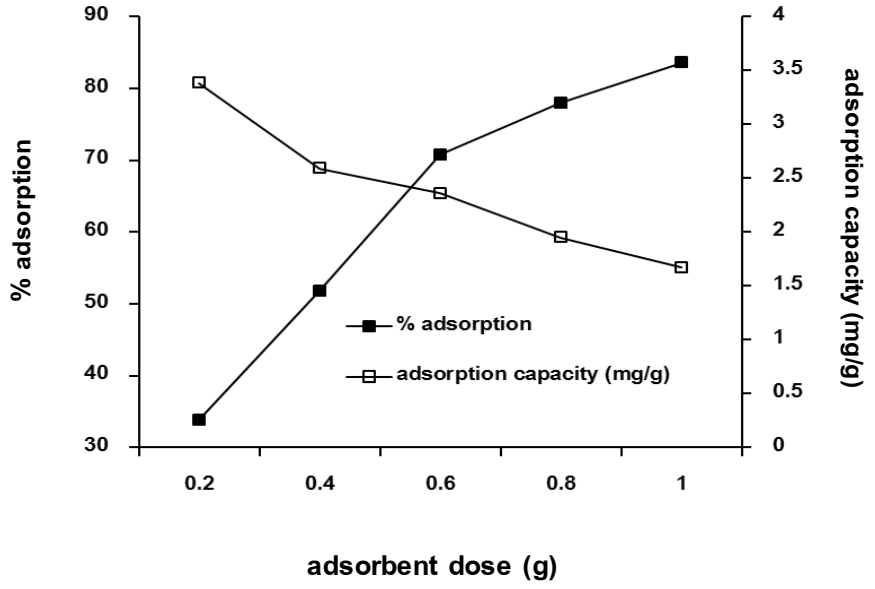

Fig 6 Effect of adsorbent dose

3.5 Effect of initial dye concentration

The effect of initial dye concentration (20 – 100 mg/L) on dye adsorption using activated carbon for the adsorbent dose of 1.0 g at pH 4 was studied. The results in Fig 7 showed that the adsorption capacity increased from 1.671 to 7.162 mg/g with increasing initial dye concentration from 20 to 100 mg/L. The adsorption capacity increased with increasing initial dye concentration because the driving force of mass transfer also increased between the aqueous solution and solid phase (Johari *et al.,* 2015). Consequently, the concentration gradient between bulk solution and adsorbent surface causes better mass transfer resulting in a larger amount being adsorbed (Bahar *et al.,* 2018). The similar observations have been reported by Sharma and Kaur (2011), Malakootian *et al*. (2016), and Bahar *et al.* (2018). However, at higher concentration (more than 80 mg/L), the rate between adsorption capacity versus concentration became lower because the active sites required for adsorption of the dye molecules will not be available (Etim *et al.,* 2016).

Food and Applied Bioscience Journal, 2020, 8(3): 1–18

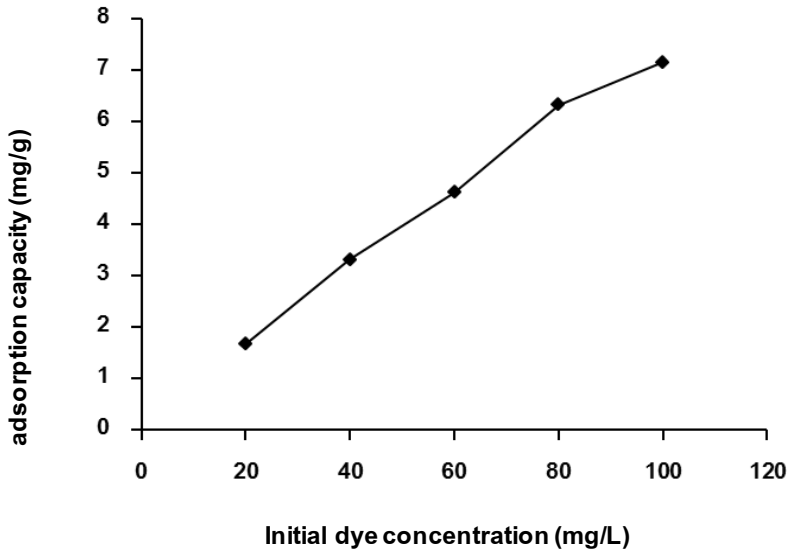

Fig 7 Effect of initial dye concentration

3.6 Adsorption isotherm

For the adsorption isotherm study, the experiments were carried out by varying initial dye concentration of 20–100 mg/L and other conditions were fixed at pH 4, contact time 120 min, and adsorbent dose 1.0 g at 30°C. The equilibrium experimental data were plotted for the linear langmuir and freundlich isotherm models (Fig 8). The calculated isotherm constants and their corresponding correlation coefficients were given in Table 1

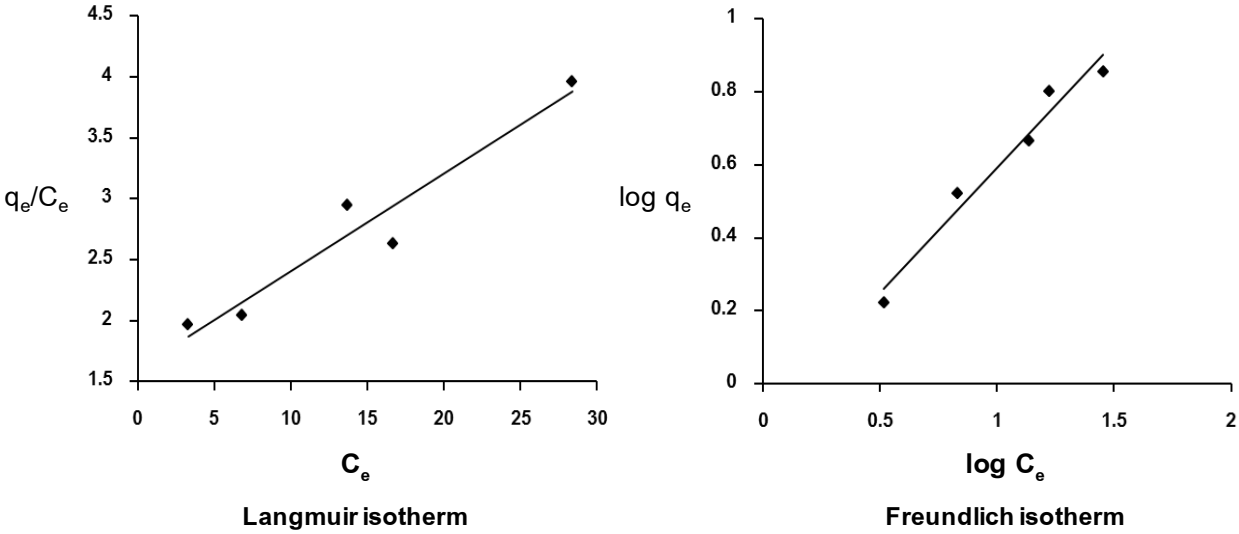

Fig 8 Langmuir and freundlich isotherm of dye adsorption onto activated carbon

Food and Applied Bioscience Journal, 2020, 8(3): 1–18

Table 1 Isotherm constants of methyl orange adsorption onto activated carbon

Langmuir isotherm				Freundlich isotherm		
q_{max} (mg/g)	K_L (L/g)	R_L	R^2	1/n	K_F (L/g)	R^2
12.50	0.056	0.471-0.151	0.929	0.684	1.241	0.963

As seen in Table 1, the R^2 value of Freundlich isotherm (0.963) was higher than of Langmuir isotherm (0.929) which indicated the multi–layer coverage adsorption on heterogeneous distribution of active sites (Amin *et al.,* 2017). The 1/n value was 0.684. The value of 1/n below 1 reflected the favorable adsorption (Mahmoud, 2015).

For the Langmuir isotherm, the maximum adsorption capacity valued 12.50 mg/g. The R_L values were in the range 0.471–0.151, implying that the dye adsorption process onto activated carbon was favorable.

3.7 Kinetic study

The linear plots of pseudo–first order, pseudo–second order and intraparticle diffusion kinetic model were shown in Fig 9.

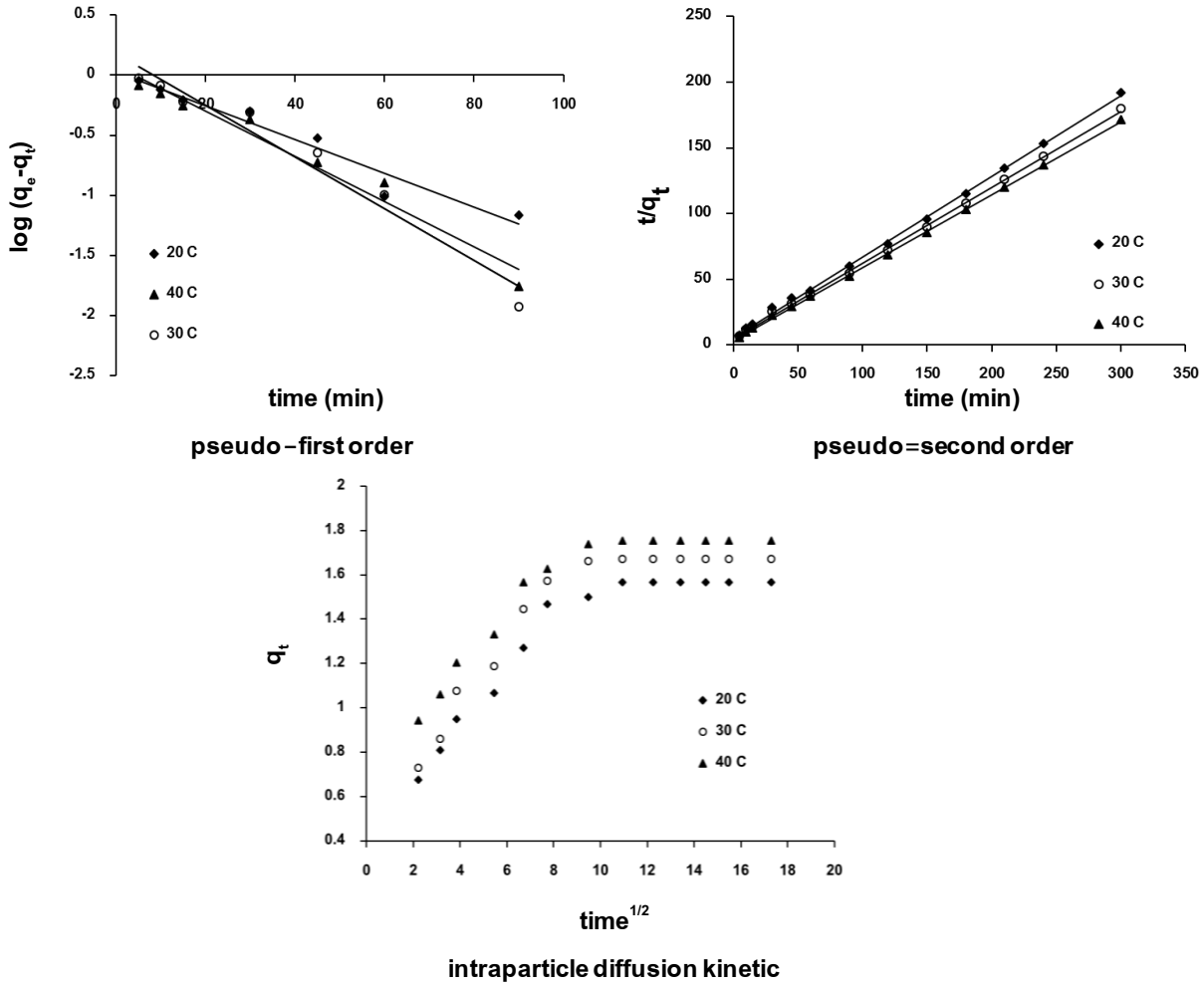

Fig 9 Kinetic models of dye adsorption on activated carbon

Food and Applied Bioscience Journal, 2020, 8(3): 1–18

The kinetic experiments of methyl orange adsorption on activated carbon were carried out at varying contact time (5–300 min) for three temperatures of 20, 30 and 40°C. From the plots seen in Fig 9, their calculated constants including the correlation coefficients (R^2) were shown in Table 2.

Table 2 Kinetic parameters of methyl orange dye adsorption onto activated carbon

Kinetic models	Temperature (°C)		
	20	**30**	**40**
q_e (exp) (mg/g)	1.565	1.671	1.753
Pseudo–first order			
q_e (cal) (mg/g)	1.064	1.509	1.183
k_1 (min^{-1})	0.032	0.050	0.043
R^2	0.950	0.962	0.966
Pseudo–second order			
q_e (cal) (mg/g)	1.634	1.735	1.804
k_2 (g./(mg.min)	0.063	0.071	0.088
R^2	0.999	0.999	0.999
Intraparticle diffusion			
C (mg/g)	0.920	0.963	1.152
K_{id} (mg/g $min^{1/2}$)	0.061	0.075	0.062
R^2	0.796	0.940	0.999

The correlation coefficients (R^2) for the dye adsorption were 0.950, 0.962 and 0.966 for pseudo–first order and 0.999, 0.999 and 0.999 for pseudo–second order at 20, 30 and 40°C, respectively. The dye adsorption data were well described by pseudo–second order model at all temperatures and its calculated adsorption capacity values (q_e,cal = 1.634, 1.735, and 1.804 mg/g) were closer to the experimental data (q_e,exp = 1.565, 1.671, and 1.753 mg/g). The pseudo–second order model was based on the assumption that the reaction was chemisorption, involving valence force or exchange of electron between adsorbent and adsorbate (Bhattacharyya and Sharma, 2005). The similar observations have been reported in the literature by Chen *et al.* (2010), Sawasdee and Watcharabundit (2016), Yu *et al.* (2018), and Phetrak *et al.*, 2019).

From the plot of the intraparticle diffusion in Fig 9, its plot showed three stages of adsorption but the linear plot did not pass through the origin, indicating that the intraparticle diffusion was not the only rate controlling step. This confirmed that the dye adsorption onto activated carbon involved the adsorption on the external surface and diffusion into the interior (Kumar and Kumaran, 2005 and Pathania *et al.,* 2017).

Food and Applied Bioscience Journal, 2020, 8(3): 1–18

3.8 Thermodynamic study

Thermodynamic parameters such as ΔG, ΔH, and ΔS of dye adsorption onto activated carbon were determined at temperature of 20–40℃ with the control of dye concentration (20 mg/L), pH (4), contact time (120 min), and adsorbent dose (1.0 g). The results showed that the adsorption capacity increased from 1.590 to 1.833 mg/g at 20 to 40℃, respectively. This may be due to the adsorption is favorable with increase temperature, indicating that the adsorption was endothermic process. The plot of log (q_e / C_e) versus 1/T was shown in Fig 10.

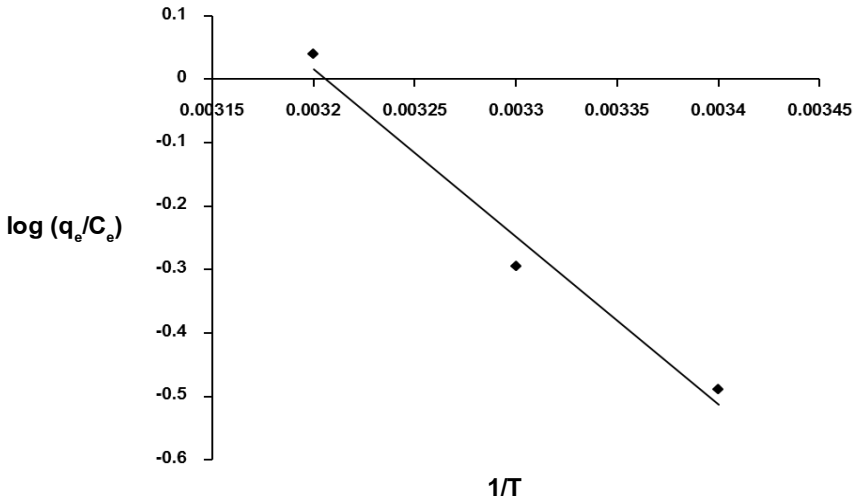

Fig 10 Van't Hoff plots of the dye adsorption onto activated carbon

As seen in Fig 9, the plot offered a straight line, and the values of ΔS and ΔH could be obtained from its intercept and slope, respectively. Thermodynamic parameters of dye adsorption onto activated carbon were shown in Table 3.

Table 3 Thermodynamic parameters of dye adsorption onto activated carbon

Temperature (°C)	ΔG (kJ/moL)	ΔH (kJ/moL)	ΔS (kJ/moL)
20	2.746		
30	1.707	50.644	0.162
40	−0.236		

In Table 3, the ΔG value decreased with an increase in temperature, suggesting that the dye adsorption increased with rising in temperature, which favored the adsorption process (Sharma *et al.,* 2010). The negative values of the ΔG confirmed the feasibility and the spontaneous. Generally, the Gibbs free energy changes for physical and chemical adsorption

are in the range of 0.0 to −20 kJ/mol and −80 to −400 kJ/moL, respectively (Li *et al.,* 2014). Therefore, the adsorption of the dye onto activated carbon could be considered for physisorption which was the predominant mechanism in the adsorption process. The positive ΔH value indicated the endothermic nature of the process, which was supported by the increase of adsorption capacity when the temperature increased. The positive ΔS value indicated that there was an increased disorder at the solid/liquid interface during dye adsorption onto the activated carbon.

4. Conclusion

In this study, the adsorption of methyl orange onto activated carbon prepared from sugarcane leaves was performed in the batch process at 30℃. The results showed that the adsorption capacity increased relatively to increase the contact time and the adsorption reached equilibrium at 120 min. In the adsorption isotherm study, the results indicated that the Freundlich model described the adsorption extremely well. The kinetic studies showed that the adsorption followed pseudo−second order kinetics. The negative value of ΔG indicated that the adsorption process was spontaneous at higher temperature. The positive value of ΔH revealed that the adsorption was an endothermic process. The positive value of ΔS suggested that the increased randomness occurred at the solid/solution interface during the dye adsorption onto activated carbon. The results in this study showed that the activated carbon was the good adsorbent for anionic dye removal in aqueous solution.

References

Ai, L., Zhang, C. and Meng, L. 2011. Adsorption of methyl orange from aqueous solution on hydrothermal synthesized Mg−Al layered double hydroxide. Journal of Chemical & Engineering Data. 56, 4217−4225.

Alau, K. K., Gimba, C. E., Agbaji, B. E. and Abeche, S. E. 2015. Structural and microstructural properties of neem husk and seed carbon activated with zinc chloride and phosphoric acid. Journal of Chemical and Pharmaceutical Research. 7(3): 2470−2479.

Albroomi, H.I., Elsayed, M. A., Baraka, A. and Abdelmaged, M. A. 2017. Batch and fixed-bed adsorption of tartrazine azo-dye onto activated carbon prepared from apricot stones. Applied Water Science. 7:2063–2074.

Amin, M. T., Alazba, A. A. and Shafiq, M. 2017. Non−spontaneous and multilayer adsorption of malachite green dye by *Acacia nilotica* waste with dominance of physisorption. Water Science & Technology. 76(7): 1805−1815.

Bahar, M. M., Mahbub, K. R., Naidu, R. and Megharaj, M. 2018. As(V) removal from aqueous solution using a low–cost adsorbent coir pith ash: equilibrium and kinetic study. Environmental Technology & Innovation. 9: 198–209.

Bamroongwongdee, C., Gaewkhem, S. and Siritrakul, P. 2018. Kinetics, equilibrium, and thermodynamics of methyl orange adsorption onto modified rice husk. KMUTNB: International Journal of Applied Science and Technology. 11(3): 185–19.

Bhattacharyya, K.G., Sharma, A., 2005. Kinetics and thermodynamics of methylene blue sorption on neem (*azadirachta indica*) leaf powder. Dyes Pigment. 65: 51–59.

Chen, S., Zhang, J., Zhang, C., Yan Li. and Li, C. 2010. Equilibrium and kinetic studies of methyl orange and methyl violet adsorption on activated carbon derived from *phragmites australis*. Desalination. 252: 149–156.

Crini, G., Peindy, H. N., Gimbert, F. and Robert, C. (2007). Removal of C.I. Basic Green 4 (Malachite Green) from aqueous solutions by adsorption using cyclodextrin–based adsorbent: Kinetic and equilibrium studies. Separation and Purification Technology. 53: 97–110.

Daneshvar, E., Sohrabi, M. S., Kousha, M., Bhatnagar, A., Aliakbarian, B., Converti, A. and Norrstrom, A.C. 2014. Shrimp shell as an efficient bioadsorbent for acid blue 25 dye removal from aqueous solution. Journal of the Taiwan Institute of Chemical Engineers. 45(6): 2926–2934.

Deng, H., Li, G., Yang, H., Tang, J. and Tang, J. 2010. Preparation of activated carbons from cotton stalk by microwave assisted KOH and K_2CO_3 activation. Chemical Engineering Journal. 163: 373–381.

Etim, U. J., Umoren, S. A. and Eduok, U. M. 2016. Coconut coir dust as a low cost adsorbent for the removal of cationic dye from aqueous solution. Journal of Saudi Chemical Society. 20: S67–S76.

Foo, K. Y and Hameed, B. H. 2012. Porous structure and adsorptive properties of pineapple peel based activated carbons prepared via microwave assisted KOH and K_2CO_3 activation. Microporous and Mesoporous Materials. 148: 191–195.

Jayganesh, D., Tamilarasan, R., Kumar, M., Murugavelu , M. and Sivakumar, V. 2018. Preparation of Eco-friendly and Low-cost Activated Carbon from *Gracilaria corticata* Seaweeds for the Removal of Crystal Violet Dye from Aqueous Solution: Equilibrium and Modeling Studies. Chiang Mai Journal of Science. 45(2): 1039–1051.

Johari, K., Saman, N., Song, S. T. and Mat, H. 2015. Adsorption equilibrium and kinetics of elemental mercury onto coconut pith. Journal of Environmental Science and Technology. 8: 74–82.

Hui, T. S. and Zaini, M. A. A. 2015. Potassium hydroxide activation of activated carbon: a commentary. Carbon Letters. 16(4): 275–280.

Khan, M. M. R., Ray, M. and Guha, A. K. 2011. Mechanistic studies on the binding of acid yellow 99 on coir pith. Bioresource Technology.102: 2394–2399.

Kumar, K. V., Kumaran, A., 2005. Removal of Methylene blue by mango seed kernel powder. Biochemical Engineering Journal. 27: 83–93.

Li, S., Han, K., Li, J., Li, M. and Lu, C. 2017. Preparation and characterization of super activated carbon produced from gulfweed by KOH activation. Microporous and Mesoporous Materials 243: 291–300.

Li, Y., Meng, F. and Zhou, Y. 2014. Adsorption behavior of acid bordeaux b from aqueous solution onto waste biomass of *enteromorpha prolifera*. Polish Journal of Environmental Studies. 23(3): 783–792.

Liang, S., Guo, X., Feng, N. and Tian, Q., 2010. Isotherms, kinetics and thermodynamic studies of adsorption of Cu^{2+} from aqueous solutions by Mg^{2+}/K^{+} type orange peel adsorbent. Journal of Hazardous Materials. 174: 756–762.

Mahmoud, M. A. 2015. Kinetics and thermodynamics of aluminum oxide nanopowder as adsorbent for Fe (III) from aqueous solution. Beni-Suef University Journal of Basic and Applied Sciences. 4: 142–149.

Malakootian, M., Mahvi, A.H., Mansoorian, H.J. and Khanjani, N. 2018. Agrowaste Based Ecofriendly Bio-adsorbent for the Removal of Phenol: Adsorption and Kinetic Study by *Acacia tortilis* Pod Shell. Chiang Mai Journal of Science. 45(1): 355–368.

Ngulube, T., Gumbo, J. R., Masindi, V. and Maity, A. 2018. Calcined magnesite as an adsorbent for cationic and anionic dyes: characterization, adsorption parameters, isotherms and kinetics study. Heliyon. 4(10): doi: 10.1016/j.heliyon.2018. e00838.

Nsami, J. N. and Mbadcam, J. K. 2013. The Adsorption Efficiency of Chemically Prepared Activated Carbon from Cola Nut Shells by $ZnCl_2$ on Methylene Blue. Journal of Chemistry. Vol. 2013. Article ID 469170. 7 pages. http://dx.doi.org/10.1155/2013/469170.

Pathania, D., Sharma, S. and Singh, P. 2017. Removal of methylene blue by adsorption onto activated carbon developed from *Ficus carica* bast. Arabian Journal of Chemistry. 10: S1445–S1451.

Phetrak, A., Sangkarak, S., Ampawong, S., Ittisupornrat,S. and Phihusut, D. 2019. Kinetic Adsorption of Hazardous Methylene Blue from Aqueous Solution onto Iron-Impregnated Powdered Activated Carbon. Environment and Natural Resources Journal. 17(4): 78–86.

Saad, M. J., Chia, C.H., Zakaria, S., Sajab, M. S., Misran, S., Rahman, M.H.A. AND Xian, S. 2019. Physical and chemical properties of the rice straw activated carbon produced from carbonization and KOH activation processes. Sains Malaysiana. 48(2): 385–391. ISSN 0126–6039.

Shao, H., Li, Y., Zheng, L., Chen, T. and Liu, J. 2017. Removal of methylene blue by chemically modified defatted brown algae *Laminaria japonica*. Journal of the Taiwan Institute of Chemical Engineers. 80: 525–532.

Sharma, P and Kaur, H. 2011. Sugarcane bagasse for the removal of erythrosin B and methylene blue from aqueous waste. Applied Water Science. 1: 135–145.

Sharma, P., Kaur, R., Baskar, C. and Chung, W. 2010. Removal of methylene blue from aqueous waste using rice husk and rice husk ash. Desalination. 259(1–3): 249–57.

Sawasdee, S and Watcharabundit, P. 2016. Effect of Temperature on Brilliant Green Adsorption by Shrimp Shell: Equilibrium and Kinetics. Chiang Mai University Journal of Natural Sciences. 15(3): 221–236.

Yakout, S. M., Hassan, M. R., El–Zaidy, M. E., and Shair, O. H., and Salih, A. M. 2019. Kinetics of methyl orange adsorption on activated carbon derived from pine (*Pinus Strobus*) sawdust. BioResources. 14(2): 4560–4574.

Yu, J., Zhang, X., Wang, D. and Li, P. 2018. Adsorption of methyl orange dye onto biochar adsorbent prepared from chicken manure. Water Science & Technology. 77(5): 1303–1312.